

An Elusive Intermediate Uncovered in the Pathway for Electrochemical Carbon Dioxide Reduction by Ruthenium Polypyridyl Catalysts – A Combined Spectroscopic and Computational Investigation

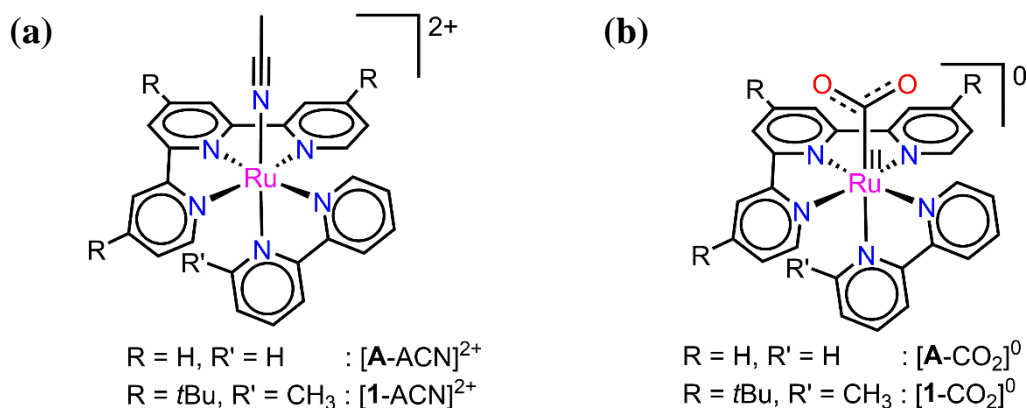
ABSTRACT: A scrupulous study of the catalytic cycle for electrochemical CO₂ reduction by the ruthenium 2,2':6',2''-terpyridine (tpy) 2,2'-bipyridine (bpy) class of catalysts is presented. An unprecedented η^2 -(C,O')-carboxycarboxylatoruthenium(II) metalacyclic intermediate, critical for C-O bond dissociation at low overpotentials, so **far** precluded from mechanistic considerations of polypyridyl transition metal complex catalysts, is unearthed by infra-red spectroscopy coupled to controlled potential electrolysis in corroboration with density functional theory (DFT) investigations. Thermodynamic and kinetic analyses of the intermediate reveal the important role of the structural flexibility of polypyridyl ligands and fine electronic tunability of the metal center, along with kinetic *trans effect*, in propelling catalysis at lower overpotentials. The choice of metal center, Ru in the present case, points to the fact that the requirement of an additional Lewis acid to enhance C-O bond dissociation, hence increase the catalytic rate or turnover, can be circumvented.

Electrochemical reduction of CO₂ to CO (eCRR) is an attractive reaction as it can assist in mitigating atmospheric CO₂, it is a step for storage of renewable energy in energy dense materials, and CO itself has wide use as a synthetic reagent in the chemical industry. While the reaction has a thermodynamic potential of -1.28 V vs Fc⁺/Fc under standard conditions, it typically suffers from too high overpotentials for efficient implementations. The overpotentials can largely be tracked to a few kinetically slow steps, that require excessive reduction of the catalytic center. On molecular catalysts there are three key steps that have been identified and modification of the catalyst structure has been focused on enhancing the rates of these steps: 1)

CO₂ binding to the catalyst 2) the C-O cleavage 3) CO dissociation. Another concern for molecular catalysts is the stability, which is typically addressed by using multidentate ligands, such as polypyridyl ligands or porphyrins. Of the three steps listed we focus on the C-O cleavage step herein. Normally, additional reduction on the metal or ligand can facilitate the C-O cleavage but will typically occur at very negative potentials, thus leading to high overpotentials. In nature the carbon monoxide dehydrogenase enzymes (CODH) can efficiently and reversibly convert CO to CO₂. In the active site of CODH there is a Ni/Fe/S cluster where the Ni is the redox and chemically active center. In close proximity is a redox inactive Fe(III) Lewis acidic center that facilitates the C-O cleavage by stabilizing a dissociating OH⁻ group. This function has been mimicked in artificial systems, *e.g.* by Buss et al. who found that introduction of fluorinated triaryl boranes led to enhancement of proton assisted C-O cleavage (JACS 2018, 10121–10125). Hong et al. reported a Ni(II) complex where a Lewis acid was incorporated in the coordination structure of the complex through binding of metal ions to non-coordinated pyridyl groups. Divalent ions led to ten times higher CO yields compared to the complex without ions. There are also several examples of metal complexes with Brønsted acidic groups positioned close to the reactive center that have been proposed to facilitate the C-O cleavage. (*Science* 2012, 338, 90-94, *Chem. – Eur. J.*, 2017, 23(20), 4782–4793, *ACS Cent. Sci.*, 2018, 4(3), 397–404, *J. Am. Chem. Soc.*, 2017, 139(7), 2604–2618, *Inorg. Chem.*, 2015, 54(11), 5285–5294, *Dalton Trans.*, 2019, 48, 12730-12737).

In the current report we have identified a way to facilitate the C-O bond cleavage step that does not require additional reduction of the catalyst, no external Lewis acid, and can proceed in absence of protic solvent or ligands. The catalyst is the recently reported [Ru(*t*Bu₃tpy)(*m*-CH₃bpy)MeCN]²⁺ complex, which we recently showed to be an active CO₂ to CO reduction catalyst already at the first reduction peak. We have identified a key intermediate using a

combination of spectroscopic and computational methods. A key feature of the catalyst is the hemilabile bonding of the ligands that create enough stability, without hampering two-site reactivity.



Scheme 1. Pictorial representation of (a) complexes [A-ACN]²⁺ and [1-ACN]²⁺, (b) the metal-η¹-C-carboxylate intermediate [Ru^{II}-CO₂²⁻]⁰.

Meyer *et al.* proposed that the tpy-bpy analogue complex forms a [A-CO₂]⁰ intermediate after two reductions and exchange of a solvent ligand for CO₂ (Scheme 1). It was proposed to then undergo the addition of a third electron onto the tpy in the next step of the catalytic cycle.⁶ We computed the potential for the addition of a third electron onto the similar [1-CO₂]⁰ to -2.52 V (vs. Fc^{+/0}), indicating that this reduction is unlikely at an applied potential of -1.82 V¹⁹, which is the cathodic peak potential at 0.2 V s⁻¹ under CO₂. An alternative reaction involves another CO₂ molecule that form a bond to the electron-rich oxygen of the Ru-bound CO₂ in [1-CO₂]⁰ in a “head-to-tail”⁴¹ fashion. The activation energy (ΔG[‡]) for this step is calculated to be 15.4 kcal mol⁻¹, the reaction free energy 8.0 kcal mol⁻¹ (Scheme S1). The activation free energy indicates a rapid reaction; however, the reaction free energy indicates that the product complex could be part of the mechanism but should not be detectable.

The IR spectrum in our previous report of a bulk electrolyzed 1.0 mM solution of [1-ACN](PF₆)₂ in anhydrous CH₃CN under CO₂ (0.28 M) (Figure S6),¹⁹ displays the evolution of three major peaks centered at 1684 cm⁻¹, 1645 cm⁻¹ and 1304 cm⁻¹. The peaks were assigned to the CO₃²⁻/HCO₃²⁻ in CH₃CN.^{19,42} A weak shoulder at 1740 cm⁻¹ along with some unresolvable structured transitions near 1250 cm⁻¹ evolves as the reaction proceeded (Figure S6). The calculated spectra of [1-CO₂]⁰ has a peak at 1701 cm⁻¹, while [1-CO₂CO₂]⁰ has a peak 1784 cm⁻¹. The observed shoulder at 1740 cm⁻¹ falls in between the calculated structures and likely belong to a different species. We therefore studied the potential steps after the formation of [1-CO₂CO₂]⁰.

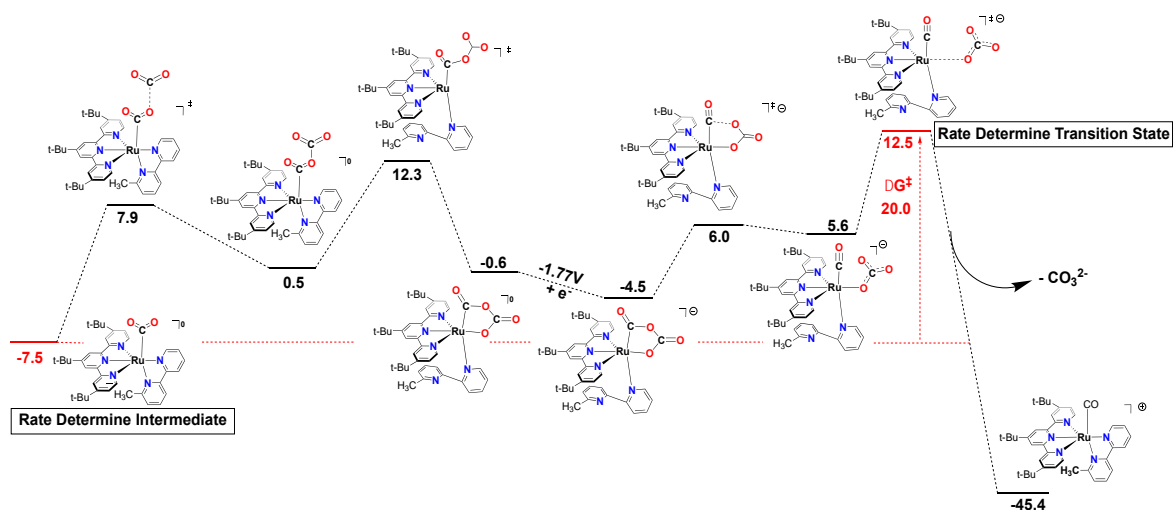
A possible route from [1-CO₂CO₂]⁰ is direct C-O bond dissociation, producing CO₃²⁻ and the carbonyl complex (Scheme S2(a)). However, the calculated ΔG^\ddagger for this reaction is extremely high (60.5 kcal mol⁻¹). After a second CO₂ has bonded [1-CO₂CO₂]⁰ can be expected to be more electrophilic than [1-CO₂]⁰ and could be reduced at a less negative potential. However, our calculated potential -2.13 V (vs. Fc^{+/0}) is higher than the applied potential indicating that some other process is operating. The negatively charged terminal oxygen in [1-CO₂CO₂]⁰ could attack the Ru center in another vicinal 5-coordinate intermediate [1]⁺, the latter obtained by dissociation of CH₃CN on [1-ACN]²⁺,¹⁹ forming a bimetallic intermediate with -C(O)O-C(O)O- bridge (Scheme S2(b)), similar to one proposed for Re^I(bpy)(CO)₃X catalysts.^{7,12,43} However, this scenario is unlikely given that the catalytic current shows a first order dependence on the concentration of the catalyst in the range 0.05 mM to 1.0 mM.¹⁹ Therefore the last alternative left is structural re-organization of the complex, either to facilitate C-O bond cleavage or to drive the subsequent reduction at a more positive potential. In [1-COOCO₂]⁰ both the -CO₂CO₂ ligand and the 6-Mebpy are potential bidentate ligands. We explored the ligand exchange of the equatorial nitrogen of 6-Mebpy for the terminal oxygen of -CO₂CO₂.

The reaction was found to have a ΔG^\ddagger of 11.8 kcal mol⁻¹ relative to [1-CO₂CO₂]⁰ giving an overall activation energy of 19.8 kcal mol⁻¹ relative to [1-CO₂]⁰. The optimized structure of [1-CO₂CO₂]^{0,c} (Figure S9(a)) displays non-coplanarity of the *py* and *py*^{Me} rings with respect to each other, the interplanar angle (N4-Cb-Cb'-N5 dihedral; Table S3) being 22.7°, due to the steric repulsion between *py*^{Me} and *t*Bu₃tpy. [1-CO₂CO₂]^{0,c} is more stable than [1-CO₂CO₂]⁰ by 1.1 kcal mol⁻¹ (Scheme 3). A similar partial de-coordination and rotation around the C-C' bond of 2,2'-bipyridine (bpy) fragment of a hexadentate ligand in a Co complex was proposed by Lucarini *et al.*⁴⁴ The structural flexibility of 6-Mebpy, in combination with the steric clash between the -CH₃ (on 6-Mebpy) and *t*Bu₃tpy in makes the rearrangement facile in our case. There are a few examples 5-membered metallacycles from two CO₂ molecules as in [1-CO₂CO₂]^{0,c},⁴⁵⁻⁵¹ albeit with phosphorous containing ligands only and manifesting *stoichiometric* activation of CO₂.

Despite being 1.4 kcal more stable than [1-CO₂CO₂]^{0,c,t} (*i.e.* when a Ru-tpy bond breaks), the calculated spectra of [1-CO₂CO₂]^{0,c,b} (*i.e.* when a Ru-bpy bond breaks) does not have the peak in the 1740 cm⁻¹ region that shows on the experimental IR. The DFT calculated IR spectrum of [1-CO₂CO₂]^{0,c} (Figure S8(b)) displays a strong peak at 1747 cm⁻¹, which corresponds to the symmetric C=O stretch (Figure S8(c)), along with less intense peaks at 1642 and 1258 cm⁻¹, corresponding to the asymmetric C=O stretch and a C-O stretch, respectively. The first peak agrees well with experimentally observed shoulder at 1740 cm⁻¹ and the peak at 1258 cm⁻¹ corresponds well to the smaller peak at 1250 cm⁻¹.

Still the calculated Gibbs free energy of [1-CO₂CO₂]^{0,c} is relatively high indicating that it is not observable. We also considered the possible reduction of [1-CO₂CO₂]^{0,c} to [1-CO₂CO₂]^{-1,c}. The potential was calculated to merely -1.77 V which makes it more likely to observed at the applied potential, with a calculated free energy of 3.5 kcal mol⁻¹ relative to [1-CO₂]⁰. The structure of

the reduced complex $[\mathbf{1}\text{-CO}_2\text{CO}_2]^{-1,c}$ is similar to $[\mathbf{1}\text{-CO}_2\text{CO}_2]^{0,c}$ but with a broken bond to the bipyridine which is just weakly interacting with the catalyst. The IR spectra of $[\mathbf{1}\text{-CO}_2\text{CO}_2]^{-1,c}$ has very similar features as that of $[\mathbf{1}\text{-CO}_2\text{CO}_2]^{0,c}$ with peaks at 1744cm^{-1} , 1688cm^{-1} , and 1287cm^{-1} , corresponding well to the experimental spectrum.

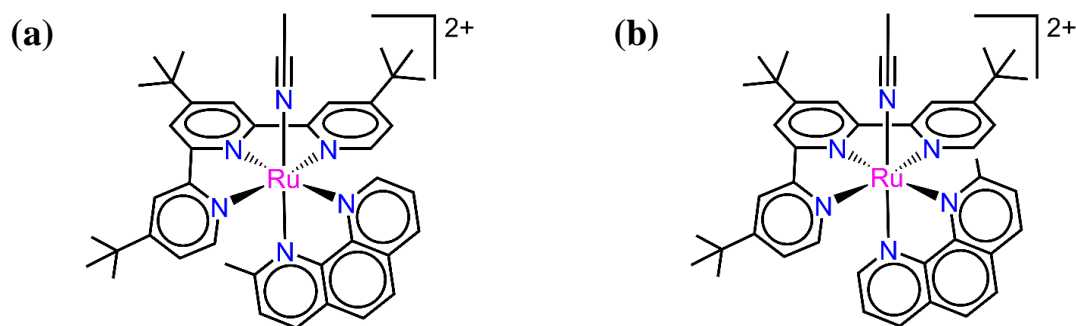


Scheme 3. Pathway to CO_3^{2-} via the cyclic two-electron reduced intermediate $[\mathbf{1}\text{-COOCO}_2]^{0,c}$.

The structure of $[\mathbf{1}\text{-CO}_2\text{CO}_2]^{-1,c}$ has some interesting features that could have implications for the C-O cleavage. Compared to the non-cyclic $[\mathbf{1}\text{-CO}_2\text{CO}_2]^0$, where C-O cleavage has an activation energy of $60.5\text{ kcal mol}^{-1}$, the C-O bond that will be cleaved is elongated from 1.36\AA to 1.42\AA indicating more single bond character. We located a transition state for the C-O cleavage just $10.5\text{ kcal mol}^{-1}$ above $[\mathbf{1}\text{-CO}_2\text{CO}_2]^{-1,c}$ resulting in $[\mathbf{1}(\text{CO})(\text{OCO}_2)]^{-1}$, where the Ru-N distance is very long at 2.7\AA but some interaction can be seen, at $13.1\text{ kcal mol}^{-1}$ relative to $[\mathbf{1}\text{-CO}_2]^0$. Dissociation of carbonate then proceeds with an activation energy at $20.0\text{ kcal mol}^{-1}$, which is accompanied with reformation of the Ru-bpy interaction. It appears that not only does the $[\mathbf{1}\text{-CO}_2\text{CO}_2]^{-1,c}$ form, it leads to very facilitated C-O cleavage by weakening of the C-O single bond. The weakening is induced by the Lewis acidic nature of the site of oxygen

coordination at Ru, and hence, Ru acts as both a Lewis base in the formation of the Ru-C bond and a Lewis acid in the formation of the Ru-O-bond. It is likely that the formation of the metallacycle also induces some strain, that further weakens the C-O bond, as evidenced by the small O-Ru-C angle of 78.8° in $[\mathbf{1}\text{-CO}_2\text{CO}_2]^{-1,c}$. In scheme 3 the reaction from $[\mathbf{1}\text{-CO}_2\text{CO}_2]^0$ to $[\mathbf{1}\text{-CO}]^{-1}$ is outlined. The highest point is the formation of $[\mathbf{1}\text{-CO}_2\text{CO}_2]^{0,c}$ at $19.1 \text{ kcal mol}^{-1}$ but with the dissociation of carbonate transition state at a similar free energy of $X.X \text{ kcal mol}^{-1}$. The experimental TOF of 1.14 s^{-1} corresponds to an activation free energy of $17.5 \text{ kcal mol}^{-1}$, in good agreement with our calculated number.

A key to the potential involvement of $[\mathbf{1}\text{-CO}_2\text{CO}_2]^{-1,c}$ in the mechanism is the hemi-labile coordination of the 6-Mebpy ligand. To test its involvement we synthesized a complex where the 6-Mebpy was replaced by 2-Mephen. It is well known that 1,10-phenanthroline (phen) forms more stable metal complexes compared to bpy.



Scheme 4. Pictorial representation of $[\mathbf{2}\text{-ACN}]^{2+}$: (a) *distal* isomer, (b) *proximal* isomer.

Complex $[\mathbf{2}\text{-ACN}](\text{PF}_6)_2$ was synthesized following the same protocol as for $[\mathbf{1}\text{-ACN}](\text{PF}_6)_2$ (see Experimental Section for details). The NMR spectrum (Figure S4) of the complex indicates its diamagnetic nature, as well as the presence of both *proximal* and *distal* isomers. The cyclic voltammogram (CV) of $[\mathbf{2}\text{-ACN}](\text{PF}_6)_2$ displayed four one-electron redox waves, ox1, red1, red2 and red3, under Ar (Figure S10, Table S4). The red2 and red3 waves become reversible at scan rates above 0.75 Vs^{-1} (Figure S10(b), Table S4(b)). The reversibility of the wave at first

reduction, red1 ($E_{p,c} = -1.82$ V (vs. $\text{Fc}^{+/0}$)), under Ar was lost under CO_2 (0.28 M)⁵⁵, with concomitant enhancement in cathodic current; $\frac{i_{p,c}(\text{CO}_2)}{i_{p,c}(\text{Ar})} \approx 2$, where $i_{p,c}(\text{CO}_2)$ and $i_{p,c}(\text{Ar})$ represent the cathodic peak currents under CO_2 and Ar respectively (Figure 3). The current increase under CO_2 at the first reduction was however less than it was for $[\mathbf{1}\text{-ACN}](\text{PF}_6)_2$, the latter exhibiting $\frac{i_{p,c}(\text{CO}_2)}{i_{p,c}(\text{Ar})} \approx 4$.¹⁹ The cathodic currents under CO_2 increased further at more negative potentials (Figure S11).

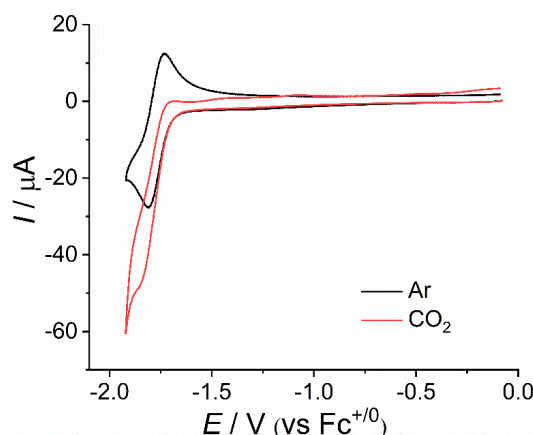


Figure 3. Cyclic voltammograms displaying the redox waves at first reduction for a 1.0 mM solution of $[\mathbf{2}\text{-ACN}](\text{PF}_6)_2$ under Ar (black) and CO_2 (red) at 0.2 V s^{-1} .

Initially, we were surprised by the current enhancement of $[\mathbf{2}\text{-ACN}](\text{PF}_6)_2$ under CO_2 . We therefore recorded the time evolved IR spectra during the CPE of $[\mathbf{2}\text{-ACN}](\text{PF}_6)_2$ at -1.82 V (vs. $\text{Fc}^{+/0}$) under CO_2 (0.28 M), which displayed the evolution of bands at 1735 , 1612 and 1272 cm^{-1} along with 1686 , 1645 , and 1302 cm^{-1} (Figure 4), the latter three being present in case of $[\mathbf{1}\text{-ACN}](\text{PF}_6)_2$ as well.¹⁹ The bands are thus very similar to the bands of $[\mathbf{1}\text{-CO}_2\text{CO}_2]^{0,c}$ and $[\mathbf{1}\text{-CO}_2\text{CO}_2]^{-1,c}$, despite the blocking of the potential decoordination of the equatorial nitrogen. It is however possible that the terpyridine ring has similar hemi-lability. We optimized the structure of $[\mathbf{2}\text{-COOCO}_2]^{0,c}$ (Figure S9(c)). Its calculated IR spectrum in CH_3CN displays peaks at 1746 (symmetric C=O stretches), 1690 (asymmetric C=O stretches), and 1257 (C-O stretches) cm^{-1} (Figures S12 and S8(c)), which correspond well to the experimentally obtained bands at

1735, 1686, and 1272 cm^{-1} (Figure 4) respectively. Further support for the assignment of these IR bands to the metalacyclic intermediate comes from the complex $\text{Ir}(\text{PMe}_3)_3(\text{Cl})(\text{COOCOO})$, reported by Herskovitz *et. al.*,⁴⁵ incorporating a $(\eta^2\text{-C,O'})\text{Ir}$ cycle similar to the one proposed in the present work. It was the first complex reported to possess two CO_2 molecules in a “head-to-tail” arrangement, made by stoichiometric and reversible CO_2 activation. It exhibited IR bands at 1725, 1680, 1648 (sh), 1605, and 1290 cm^{-1} which were ascribed to the $-\text{C}(\text{O})\text{OC}(\text{O})\text{O}-$ moiety of the metallacycle.

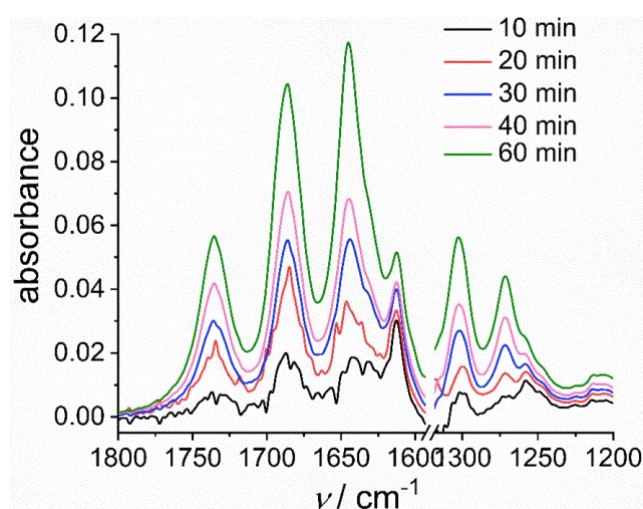


Figure 4. Fourier transformed infra-red (FT-IR) absorbance spectra of aliquots of 1 mM solution of $[\mathbf{2}\text{-ACN}](\text{PF}_6)_2$ in $\text{CH}_3\text{CN}/0.1 \text{ M TBAPF}_6$ saturated with CO_2 (0.28 M), taken during its controlled potential electrolysis at an applied potential of -1.82 V (vs. $\text{Fc}^{+/0}$) at 298 K.

The rate of C-O bond dissociation is presumably lower in $[\mathbf{2}\text{-CO}_2\text{CO}_2]^{0,c}$ than $[\mathbf{1}\text{-CO}_2\text{CO}_2]^{0,c}$ or $[\mathbf{1}\text{-COOCO}_2]^{-1,c}$, since unlike the latter two intermediates, we were able to observe the former unambiguously in the IR spectrum during CPE. Further detailed thermodynamic and kinetic investigations of the catalytic activity of $[\mathbf{2}\text{-ACN}](\text{PF}_6)_2$ towards electrochemical CO_2 reduction are underway.

The current work presents for the first time, the involvement of an unprecedented 5-membered *ruthenacyclic* intermediate in the catalytic cycle of electrochemical CO₂ reduction by Ru-polypyridyl complexes. The fine tuning of the electronic and steric properties by utilizing the *flexibility* feature of the polypyridyl ligands with respect to rotation around C-C' bonds renders the spectroscopic observation of such an intermediate possible, without destroying the structural integrity of the catalyst. This particular class of catalysts also showcases a unique example of a sole metal center performing the roles of both a Lewis base (for attachment of CO₂ *via* C atom) and a Lewis acid (for attachment of CO₂ *via* O atom), hence portraying the impressive tunability of the electronic nature of the metal center in the course of catalysis.

ASSOCIATED CONTENT

Supporting Information

The supporting information is available free of charge on the ACS Publications Website at DOI:

Experimental details, Figures, Tables

AUTHOR INFORMATION

Corresponding Authors

ORCID

Notes

The authors declare no competing financial interest.

ACKNOWLEDGEMENTS: The authors would like to acknowledge the Swedish National Infrastructure for Computing (SNIC), which is funded by the Swedish Research Council through grant agreement no.2016-07213, in Linköping (NSC) for the computational resources. The computations were performed under project number SNIC2017/1-13, SNIC2018/3-1, SNIC2019/3-6 and SNIC2020/5-41. We acknowledge NordForsk (No.85378) for the Nordic University hub NordCO₂. MA has been supported by the Swedish Research Council (VR) grant

number 2018-05396, and the Knut & Alice Wallenberg (KAW) project CATSS (KAW 2016.0072). XC acknowledges the China Scholarship Council (CSC) for financial support. Stenhagen Analyslab AB is gratefully acknowledged for mass spectral measurements.

REFERENCES

1. Elgrishi, N.; Chambers, M. B.; Wang, X.; Fontecave, M. Molecular polypyridine-based metal complexes as catalysts for the reduction of CO₂. *Chem. Soc. Rev.* **2017**, *46* (3), 761-796.
2. Francke, R.; Schille, B.; Roemelt, M. Homogeneously Catalyzed Electroreduction of Carbon Dioxide—Methods, Mechanisms, and Catalysts. *Chem. Rev.* **2018**, *118* (9), 4631-4701.
3. Queyriaux, N.; Abel, K.; Fize, J.; Pécaut, J.; Orio, M.; Hammarström, L. From non-innocent to guilty: on the role of redox-active ligands in the electro-assisted reduction of CO₂ mediated by a cobalt(II)-polypyridyl complex. *Sust. Energy & Fuels* **2020**, *4* (7), 3668-3676.
4. Bolinger, C. M.; Story, N.; Sullivan, B. P.; Meyer, T. J. Electrocatalytic reduction of carbon dioxide by 2,2'-bipyridine complexes of rhodium and iridium. *Inorg. Chem.* **1988**, *27* (25), 4582-4587.
5. Bolinger, C. M.; Sullivan, B. P.; Conrad, D.; Gilbert, J. A.; Story, N.; Meyer, T. J. Electrocatalytic reduction of CO₂ based on polypyridyl complexes of rhodium and ruthenium. *J. Chem. Soc., Chem. Commun.* **1985**, (12), 796-797.
6. Chen, Z.; Chen, C.; Weinberg, D. R.; Kang, P.; Concepcion, J. J.; Harrison, D. P.; Brookhart, M. S.; Meyer, T. J. Electrocatalytic reduction of CO₂ to CO by polypyridyl ruthenium complexes. *Chem. Commun.* **2011**, *47* (47), 12607-12609.
7. Sullivan, B. P.; Bolinger, C. M.; Conrad, D.; Vining, W. J.; Meyer, T. J. One- and two-electron pathways in the electrocatalytic reduction of CO₂ by fac-Re(bpy)(CO)₃Cl (bpy = 2,2'-bipyridine). *J. Chem. Soc., Chem. Commun.* **1985**, (20), 1414-1416.

8. Ishida, H.; Tanaka, K.; Tanaka, T. Electrochemical CO₂ reduction catalyzed by ruthenium complexes [Ru(bpy)₂(CO)₂]²⁺ and [Ru(bpy)₂(CO)Cl]⁺. Effect of pH on the formation of CO and HCOO⁻. *Organometallics* **1987**, 6 (1), 181-186.
9. Agnew, D. W.; Sampson, M. D.; Moore, C. E.; Rheingold, A. L.; Kubiak, C. P.; Figueroa, J. S. Electrochemical Properties and CO₂-Reduction Ability of m-Terphenyl Isocyanide Supported Manganese Tricarbonyl Complexes. *Inorg. Chem.* **2016**, 55 (23), 12400-12408.
10. Chabolla, S. A.; Dellamary, E. A.; Machan, C. W.; Tezcan, F. A.; Kubiak, C. P. Combined steric and electronic effects of positional substitution on dimethyl-bipyridine rhenium(I)tricarbonyl electrocatalysts for the reduction of CO₂. *Inorg. Chim. Acta* **2014**, 422, 109-113.
11. Chabolla, S. A.; Machan, C. W.; Yin, J.; Dellamary, E. A.; Sahu, S.; Gianneschi, N. C.; Gilson, M. K.; Tezcan, F. A.; Kubiak, C. P. Bio-inspired CO₂ reduction by a rhenium tricarbonyl bipyridine-based catalyst appended to amino acids and peptidic platforms: incorporating proton relays and hydrogen-bonding functional groups. *Faraday Discuss.* **2017**, 198 (0), 279-300.
12. Machan, C. W.; Chabolla, S. A.; Yin, J.; Gilson, M. K.; Tezcan, F. A.; Kubiak, C. P. Supramolecular Assembly Promotes the Electrocatalytic Reduction of Carbon Dioxide by Re(I) Bipyridine Catalysts at a Lower Overpotential. *J. Am. Chem. Soc.* **2014**, 136 (41), 14598-14607.
13. Machan, C. W.; Sampson, M. D.; Chabolla, S. A.; Dang, T.; Kubiak, C. P. Developing a Mechanistic Understanding of Molecular Electrocatalysts for CO₂ Reduction using Infrared Spectroelectrochemistry. *Organometallics* **2014**, 33 (18), 4550-4559.
14. Sampson, M. D.; Kubiak, C. P. Manganese Electrocatalysts with Bulky Bipyridine Ligands: Utilizing Lewis Acids To Promote Carbon Dioxide Reduction at Low Overpotentials. *J. Am. Chem. Soc.* **2016**, 138 (4), 1386-1393.

15. Smieja, J. M.; Kubiak, C. P. Re(bipy-*t*Bu)(CO)₃Cl—improved Catalytic Activity for Reduction of Carbon Dioxide: IR-Spectroelectrochemical and Mechanistic Studies. *Inorg. Chem.* **2010**, *49* (20), 9283-9289.
16. Zhanaidarova, A.; Steger, H.; Reineke, M. H.; Kubiak, C. P. Chelated [Zn(cyclam)]²⁺ Lewis acid improves the reactivity of the electrochemical reduction of CO₂ by Mn catalysts with bulky bipyridine ligands. *Dalton Trans.* **2017**, *46* (37), 12413-12416.
17. Elgrishi, N.; Chambers, M. B.; Artero, V.; Fontecave, M. Terpyridine complexes of first row transition metals and electrochemical reduction of CO₂ to CO. *Phys. Chem. Chem. Phys.* **2014**, *16* (27), 13635-13644.
18. Johnson, B. A.; Agarwala, H.; White, T. A.; Mijangos, E.; Maji, S.; Ott, S. Judicious Ligand Design in Ruthenium Polypyridyl CO₂ Reduction Catalysts to Enhance Reactivity by Steric and Electronic Effects. *Chem. Eur. J.* **2016**, *22* (42), 14870-14880.
19. Johnson, B. A.; Maji, S.; Agarwala, H.; White, T. A.; Mijangos, E.; Ott, S. Activating a Low Overpotential CO₂ Reduction Mechanism by a Strategic Ligand Modification on a Ruthenium Polypyridyl Catalyst. *Angew. Chem. Int. Ed.* **2016**, *55* (5), 1825-1829.
20. Ngo, K. T.; McKinnon, M.; Mahanti, B.; Narayanan, R.; Grills, D. C.; Ertem, M. Z.; Rochford, J. Turning on the Protonation-First Pathway for Electrocatalytic CO₂ Reduction by Manganese Bipyridyl Tricarbonyl Complexes. *J. Am. Chem. Soc.* **2017**, *139* (7), 2604-2618.
21. Grills, D. C.; Farrington, J. A.; Layne, B. H.; Lyman, S. V.; Mello, B. A.; Preses, J. M.; Wishart, J. F. Mechanism of the Formation of a Mn-Based CO₂ Reduction Catalyst Revealed by Pulse Radiolysis with Time-Resolved Infrared Detection. *J. Am. Chem. Soc.* **2014**, *136* (15), 5563-5566.
22. Riplinger, C.; Sampson, M. D.; Ritzmann, A. M.; Kubiak, C. P.; Carter, E. A. Mechanistic Contrasts between Manganese and Rhenium Bipyridine Electrocatalysts for the Reduction of Carbon Dioxide. *J. Am. Chem. Soc.* **2014**, *136* (46), 16285-16298.

23. Hurrell, H. C.; Mogstad, A. L.; Usifer, D. A.; Potts, K. T.; Abruna, H. D. Electrocatalytic activity of electropolymerized films of bis(vinylterpyridine)cobalt(2+) for the reduction of carbon dioxide and oxygen. *Inorg. Chem.* **1989**, 28 (6), 1080-1084.
24. Chapovetsky, A.; Do, T. H.; Haiges, R.; Takase, M. K.; Marinescu, S. C. Proton-Assisted Reduction of CO₂ by Cobalt Aminopyridine Macrocycles. *J. Am. Chem. Soc.* **2016**, 138 (18), 5765-5768.
25. Cometto, C.; Chen, L.; Lo, P.-K.; Guo, Z.; Lau, K.-C.; Anxolabéhère-Mallart, E.; Fave, C.; Lau, T.-C.; Robert, M. Highly Selective Molecular Catalysts for the CO₂-to-CO Electrochemical Conversion at Very Low Overpotential. Contrasting Fe vs Co Quaterpyridine Complexes upon Mechanistic Studies. *ACS Catal.* **2018**, 8 (4), 3411-3417.
26. Kumagai, H.; Nishikawa, T.; Koizumi, H.; Yatsu, T.; Sahara, G.; Yamazaki, Y.; Tamaki, Y.; Ishitani, O. Electrocatalytic reduction of low concentration CO₂. *Chem. Sci.* **2019**, 10 (6), 1597-1606.
27. Loipersberger, M.; Zee, D. Z.; Panetier, J. A.; Chang, C. J.; Long, J. R.; Head-Gordon, M. Computational Study of an Iron(II) Polypyridine Electrocatalyst for CO₂ Reduction: Key Roles for Intramolecular Interactions in CO₂ Binding and Proton Transfer. *Inorg. Chem.* **2020**, 59 (12), 8146-8160.
28. Sung, S.; Li, X.; Wolf, L. M.; Meeder, J. R.; Bhuvanesh, N. S.; Grice, K. A.; Panetier, J. A.; Nippe, M. Synergistic Effects of Imidazolium-Functionalization on fac-Mn(CO)₃ Bipyridine Catalyst Platforms for Electrocatalytic Carbon Dioxide Reduction. *J. Am. Chem. Soc.* **2019**, 141 (16), 6569-6582.
29. Haviv, E.; Azaiza-Dabbah, D.; Carmieli, R.; Avram, L.; Martin, J. M. L.; Neumann, R. A Thiourea Tether in the Second Coordination Sphere as a Binding Site for CO₂ and a Proton Donor Promotes the Electrochemical Reduction of CO₂ to CO Catalyzed by a Rhenium Bipyridine-Type Complex. *J. Am. Chem. Soc.* **2018**, 140 (39), 12451-12456.

30. Zee, D. Z.; Nippe, M.; King, A. E.; Chang, C. J.; Long, J. R. Tuning Second Coordination Sphere Interactions in Polypyridyl–Iron Complexes to Achieve Selective Electrocatalytic Reduction of Carbon Dioxide to Carbon Monoxide. *Inorg. Chem.* **2020**, *59* (7), 5206-5217.
31. Derrick, J.; Loipersberger, M.; Iovan, D.; Smith, P. T.; Chakarawet, K.; Long, J. R.; Head-Gordon, M.; Chang, C. J. Metal–Ligand Exchange Coupling Promotes Iron-Catalyzed Electrochemical CO₂ Reduction at Low Overpotentials **2020**. https://chemrxiv.org/articles/Metal_Ligand_Exchange_Coupling_Promotes_Iron-Catalyzed_Electrochemical_CO2_Reduction_at_Low_Overpotentials/11923176.
32. Nakada, A.; Ishitani, O. Selective Electrocatalysis of a Water-Soluble Rhenium(I) Complex for CO₂ Reduction Using Water As an Electron Donor. *ACS Catal.* **2018**, *8* (1), 354-363.
33. Gonell, S.; Lloret, J.; Miller, A. J. M. An Iron Pyridyl-Carbene Catalyst for Low Overpotential CO₂ reduction to CO: Mechanistic Comparisons with the Ruthenium Analogue and Photochemical Promotion **2020**. https://chemrxiv.org/articles/An_Iron_Pyridyl-Carbene_Catalyst_for_Low_Overpotential_CO2_reduction_to_CO_Mechanistic_Comparisons_with_the_Ruthenium_Analogue_and_Photochemical_Promotion/11911383.
34. Gonell, S.; Assaf, E. A.; Duffee, K. D.; Schauer, C. K.; Miller, A. J. M. Kinetics of the Trans Effect in Ruthenium Complexes Provide Insight into the Factors That Control Activity and Stability in CO₂ Electroreduction. *J. Am. Chem. Soc.* **2020**, *142* (19), 8980-8999.
35. Gonell, S.; Massey, M. D.; Moseley, I. P.; Schauer, C. K.; Muckerman, J. T.; Miller, A. J. M. The Trans Effect in Electrocatalytic CO₂ Reduction: Mechanistic Studies of Asymmetric Ruthenium Pyridyl-Carbene Catalysts. *J. Am. Chem. Soc.* **2019**, *141* (16), 6658-6671.
36. Elgrishi, N.; Chambers, M. B.; Fontecave, M. Turning it off! Disfavouring hydrogen evolution to enhance selectivity for CO production during homogeneous CO₂ reduction by cobalt–terpyridine complexes. *Chem. Sci.* **2015**, *6* (4), 2522-2531.

37. White, T. A.; Maji, S.; Ott, S. Mechanistic insights into electrocatalytic CO₂ reduction within [Ru^{II}(tpy)(NN)X]ⁿ⁺ architectures. *Dalton Trans.* **2014**, 43 (40), 15028-15037.
38. Hammouche, M.; Lexa, D.; Momenteau, M.; Saveant, J. M. Chemical catalysis of electrochemical reactions. Homogeneous catalysis of the electrochemical reduction of carbon dioxide by iron(0) porphyrins. Role of the addition of magnesium cations. *J. Am. Chem. Soc.* **1991**, 113 (22), 8455-8466.
39. Bhugun, I.; Lexa, D.; Savéant, J.-M. Catalysis of the Electrochemical Reduction of Carbon Dioxide by Iron(0) Porphyrins. Synergistic Effect of Lewis Acid Cations. *The Journal of Physical Chemistry* **1996**, 100 (51), 19981-19985.
40. Isegawa, M.; Sharma, A. K. CO₂ reduction by a Mn electrocatalyst in the presence of a Lewis acid: a DFT study on the reaction mechanism. *Sust. Energy & Fuels* **2019**, 3 (7), 1730-1738.
41. Nakajima, H.; Tsuge, K.; Toyohara, K.; Tanaka, K. Stabilization of [Ru(bpy)₂(CO)(η¹-CO₂)] and unprecedented reversible oxide transfer reactions from CO₃²⁻ to [Ru(bpy)₂(CO)₂]²⁺ and from [Ru(bpy)₂(CO)(η¹-CO₂)] to CO₂. *J. Organomet. Chem.* **1998**, 569 (1), 61-69.
42. Cheng, S. C.; Blaine, C. A.; Hill, M. G.; Mann, K. R. Electrochemical and IR Spectroelectrochemical Studies of the Electrocatalytic Reduction of Carbon Dioxide by [Ir₂(dimen)₄]²⁺ (dimen = 1,8-Diisocyanomenthane). *Inorg. Chem.* **1996**, 35 (26), 7704-7708.
43. Agarwal, J.; Fujita, E.; Schaefer, H. F.; Muckerman, J. T. Mechanisms for CO Production from CO₂ Using Reduced Rhenium Tricarbonyl Catalysts. *J. Am. Chem. Soc.* **2012**, 134 (11), 5180-5186.
44. Lucarini, F.; Fize, J.; Morozan, A.; Marazzi, M.; Natali, M.; Pastore, M.; Artero, V.; Ruggi, A. Insights into the mechanism of photosynthetic H₂ evolution catalyzed by a heptacoordinate cobalt complex. *Sust. Energy & Fuels* **2020**, 4 (2), 589-599.

45. Herskovitz, T.; Guggenberger, L. J. Carbon dioxide coordination chemistry. The structure and some chemistry of the novel carbon dioxide addition product chlorobis(carbon dioxide)tris(trimethylphosphine)iridium. *J. Am. Chem. Soc.* **1976**, 98 (6), 1615-1616.
46. Jurd, P. M.; Li, H. L.; Bhadbhade, M.; Field, L. D. Fe(0)-Mediated Reductive Disproportionation of CO₂. *Organometallics* **2020**, 39 (10), 2011-2018.
47. Feller, M.; Gellrich, U.; Anaby, A.; Diskin-Posner, Y.; Milstein, D. Reductive Cleavage of CO₂ by Metal–Ligand-Cooperation Mediated by an Iridium Pincer Complex. *J. Am. Chem. Soc.* **2016**, 138 (20), 6445-6454.
48. Langer, J.; Imhof, W.; Fabra, M. J.; García-Orduña, P.; Görls, H.; Lahoz, F. J.; Oro, L. A.; Westerhausen, M. Reversible CO₂ Fixation by Iridium(I) Complexes Containing Me₂PhP as Ligand. *Organometallics* **2010**, 29 (7), 1642-1651.
49. Kempe, R.; Sieler, J.; Walther, D.; Reinhold, J.; Rommel, K. Aktivierung von CO₂ an Übergangsmetallzentren: Zum Ablauf der CO₂-Reduktion an Nickel(0)-Fragmenten. *Z. Anorg. Allg. Chem.* **1993**, 619 (6), 1105-1110.
50. Dahlenburg, L.; Prengel, C. Metallorganische verbindungen des iridiums und rhodiums: XXIX. CO₂-transformationen am trisphosphanrhodium(I)-komplex Rh(4-MeC₆H₄)[*t*-BuP(CH₂CH₂CH₂PPh₂)₂]. *J. Organomet. Chem.* **1986**, 308 (1), 63-71.
51. Carmona, E.; Gonzalez, F.; Poveda, M. L.; Marin, J. M.; Atwood, J. L.; Rogers, R. D. Reaction of cis-[Mo(N₂)₂(PMe₃)₄] with carbon dioxide. Synthesis and characterization of products of disproportionation and the x-ray structure of a tetrametallic mixed-valence Mo(II)-Mo(V) carbonate with a novel mode of carbonate binding. *J. Am. Chem. Soc.* **1983**, 105 (10), 3365-3366.
52. Guadalupe, A. R.; Usifer, D. A.; Potts, K. T.; Hurrell, H. C.; Mogstad, A. E.; Abruna, H. D. Novel chemical pathways and charge-transport dynamics of electrodes modified with electropolymerized layers of [Co(v-terpy)₂]²⁺. *J. Am. Chem. Soc.* **1988**, 110 (11), 3462-3466.

53. Aroua, S.; Todorova, T. K.; Mougel, V.; Hommes, P.; Reissig, H.-U.; Fontecave, M. New Cobalt-Bisterpyridyl Catalysts for Hydrogen Evolution Reaction. *ChemCatChem* **2017**, *9* (12), 2099-2105.
54. Leung, J. J.; Warnan, J.; Ly, K. H.; Heidary, N.; Nam, D. H.; Kuehnle, M. F.; Reisner, E. Solar-driven reduction of aqueous CO₂ with a cobalt bis(terpyridine)-based photocathode. *Nature Catal.* **2019**, *2* (4), 354-365.
55. Gennaro, A.; Isse, A. A.; Vianello, E. Solubility and electrochemical determination of CO₂ in some dipolar aprotic solvents. *J. Electroanal. Chem. Interfacial Electrochem.* **1990**, *289* (1), 203-215.